

Transport of correlated electrons through disordered chains: A perspective on entanglement, conductance, and disorder averaging

Daniel Karlsson and Claudio Verdozzi

Mathematical Physics and ETSF, Lund University, 22100 Lund, Sweden

(Received 4 May 2014; revised manuscript received 13 October 2014; published 18 November 2014)

We investigate electron transport in disordered Hubbard chains contacted to macroscopic leads, via the nonequilibrium Green's function technique. We observe a crossover of currents and conductances at finite bias which depends on the relative strength of disorder and interactions. We provide a proof that the coherent potential approximation, a widely used method for treating disorder averages, fulfills particle conservation at finite bias with or without electron correlations. Finally, our results hint that the observed trends in conductance due to interactions and disorder also appear as signatures in the single-site entanglement entropy.

DOI: [10.1103/PhysRevB.90.201109](https://doi.org/10.1103/PhysRevB.90.201109)

PACS number(s): 72.15.Rn, 03.67.Mn, 71.10.Fd, 72.10.Bg

In today's quest for novel electronics and quantum-information technologies, materials with properties largely determined by electron correlations are an important asset [1]. Altogether, they exhibit a wide range of nontrivial phenomena, making them excellent potential candidates to exploit for cutting-edge functionalities and devices. However, materials behavior is often far from ideal because of uncontrolled, random inhomogeneities in the sample, i.e., disorder. Disorder can greatly affect the behavior of a solid (for example, it can dramatically alter conduction properties) and thus it should be considered in a comprehensive theoretical description [2].

Significant understanding of the behavior of noninteracting electrons in disordered solids is obtained in terms of a scaling theory of electron localization [3,4]. Interactions add great complexity to the picture, but the reverse is also true: Describing electronic correlations in the presence of sample-to-sample statistical fluctuations is much harder than for the homogenous case. For this, one can either resort to straightforward but computationally expensive sums over configurations, or to analytical treatments of statistic fluctuations such as typical medium theory [5] or the coherent potential approximation (CPA) [6,7]. Traditionally, CPA has been mostly used in static *ab initio* treatments of disordered metallic alloys [8], but, recently, it has also been used in nonequilibrium setups [9–11].

On the whole, until now rigorous understanding of interacting electrons in strongly disordered systems has come primarily from numerical studies [4,12–14] in and near equilibrium regimes, by looking, e.g., at linear conductances [15–17], spectral functions [5,18,19], the degree of localization via the inverse participation ratio [20], or signatures in the entanglement entropy [21,22].

Out of equilibrium, the situation is less defined: Even for “simple” cases such as one-dimensional (1D) wires in a quantum transport setup (for a recent review of work on 1D, see, e.g., Ref. [23]), many issues are only partially or not at all settled. For example, *how do interactions and disorder together affect conduction in a small wire when a finite electric bias is applied? And what is their effect on the entanglement in the wire in the presence of a current?*

In this Rapid Communication, we use the nonequilibrium Green's function (NEGF) technique [24,25] to address these and related questions. Specifically, we study electron transport through interacting disordered chains with Hubbard interactions and diagonal disorder (besides being of fundamental

interest, such systems are highly relevant for molecular electronics and quantum information).

Our main results are as follows: (i) Far from equilibrium, the current exhibits a nonmonotonic behavior due to the competition of disorder and interactions; (ii) for the cases considered, the interaction changes the exponential decrease of the conductance as a function of system size, typical of a noninteracting system, with a much weaker dependence; (iii) signatures of the mutual interplay of disorder and interactions can appear in the single-site entanglement entropy; and (iv) CPA is particle conserving, with or without electron correlations, and is thus suitable for nonequilibrium treatments.

Theoretical formulation. We consider short, interacting disordered chains attached to two noninteracting leads. In standard notation, the Hamiltonian is

$$H = H_{RR} + H_{LL} + H_{CC} + H_{RC} + H_{CL}, \quad (1)$$

where $R(L), C$ refer to the right (left) lead and central region, respectively. The lead Hamiltonian $H_{\alpha\alpha}$ ($\alpha = L, R$) is

$$H_{\alpha\alpha} = -J \sum_{(ij) \in \alpha, \sigma} c_{i\sigma}^\dagger c_{j\sigma} + b_\alpha \hat{N}_\alpha, \quad (2)$$

with b_α the (site-independent) bias in lead α and $J > 0$ the tunneling amplitude. The total number operator in lead α is $\hat{N}_\alpha = \sum_{i \in \alpha} \hat{n}_i$, and $\hat{n}_i = \hat{n}_{i\uparrow} + \hat{n}_{i\downarrow}$, $\hat{n}_{i\sigma} = c_{i\sigma}^\dagger c_{i\sigma}$. The chain/central region Hamiltonian H_{CC} is

$$H_{CC} = -J \sum_{(ij) \in C, \sigma} c_{i\sigma}^\dagger c_{j\sigma} + \sum_i \epsilon_i \hat{n}_i + U \sum_i \hat{n}_{i\uparrow} \hat{n}_{i\downarrow}, \quad (3)$$

where the ϵ_i 's are the (random) on-site energies of the chain, which account for disorder in the system. U is the (site-independent) contact interaction strength in the chain. In obvious notation, the leads-chain coupling is

$$H_{LC} + H_{RC} = -J (c_{1L}^\dagger c_{1C} + c_{1R}^\dagger c_{1C}) + \text{H.c.}, \quad (4)$$

i.e., the semi-infinite leads are connected to the ends of the chain. We take J to be the same everywhere, which corresponds to transparent boundary conditions, i.e., only disorder and interactions affect the electron transmission through the chain. Also, we put $J = 1$, which sets the energy scale. Furthermore, for noninteracting leads, one can solve in closed form for the NEGF in the central region

via an embedding self-energy $\Sigma_{\text{emb}} = \Sigma_L + \Sigma_R$ [26,27]. To calculate steady-state properties, we evaluate the lesser $G^<(\omega)$ and the retarded $G^R(\omega)$ Green's functions in the chain,

$$G^R(\omega) = \frac{1}{\omega + i\eta - H_0 - \Sigma^R(\omega)}, \quad (5)$$

$$G^<(\omega) = G^R(\omega)\Sigma^<(\omega)G^A(\omega), \quad (6)$$

where H_0 is the noninteracting part of Eq. (3). In the most general case, the self-energy is $\Sigma = \Sigma_{\text{HF}} + \Sigma_{\text{MB}} + \Sigma_{\text{emb}} + \Sigma_{\text{CPA}}$, i.e., the sum of Hartree-Fock, correlation, embedding, and disorder contributions, respectively. When disorder is treated via numerical configuration averaging, the Σ_{CPA} is omitted. In all our calculations, the bias is applied only to the left lead, and the leads are half filled. In the numerical configuration averaging, we study both box (uniform) disorder, $\epsilon_i \in [-W/2, W/2]$, and binary disorder, $\epsilon_i = -W/2, W/2$. For box disorder, we performed averages over at least 50 configurations, and we checked that this number is enough to produce reliable currents and densities. For binary disorder, we performed complete averages.

We use the second-Born Approximation (BA) to include correlation effects. The BA takes into account all diagrams of second order in the interaction and incorporates nonlocal effects. Exact benchmarks from small isolated clusters [28,29] and quantum transport setups [30] show that the BA is a versatile, overall fairly accurate approximation for low/intermediate interaction strengths. In the BA, for local interactions, $\Sigma_{\text{MB}}(t)$ in steady state reads

$$\Sigma_{ij}^{\text{MB}}(t) = U_i U_j \tilde{G}_{ij}(t) G_{ji}(-t) G_{ij}(t), \quad (7)$$

which, by the Langreth rules, yields expressions for $\Sigma_{\text{MB}}^<$ and Σ_{MB}^R . The density is calculated as $n_j = 2 \int_{-\infty}^{\infty} \frac{d\omega}{2\pi i} G_{jj}^<(\omega)$, and the current through lead α is obtained via the Meir-Wingreen formula [31],

$$I_\alpha = \int_{-\infty}^{\infty} \frac{d\omega}{2\pi} \text{Tr}\{\Gamma^\alpha(\omega)(G^<(\omega) - 2\pi i f_\alpha(\omega)A(\omega))\}. \quad (8)$$

The trace is taken over the central region, f_α is the ($T = 0$) Fermi distribution of lead α , and the nonequilibrium spectral function is defined as $-2\pi i A = G^R - G^A$, with $G^A = (G^R)^\dagger$, and $\Gamma^\alpha = -2 \text{Im}(\Sigma_\alpha)$. Equations (5) and (6) were solved self-consistently with the frequency integrals in the BA performed via fast Fourier transform (FFT).

Disorder versus interactions: Results. In Fig. 1, we illustrate the dependence of the averaged current in the steady state on the strength of disorder W and interactions U . Results are for a chain of $L = 10$ sites, and bias $b_L = 0.5$. Starting with Fig. 1(a), we note that the current has a different qualitative behavior in different regions of the U - W plane. In fact, close to the no-interaction (no-disorder) line the current decreases monotonically as a function of disorder (interactions). However, as shown in the current heat map, for intermediate interactions and/or disorder (relative the scale considered), the current clearly exhibits nonmonotonic behavior at finite bias. The behavior is clearly depicted in Fig. 1(b): As a function of W , the region of nonmonotonic behavior for the current moves to higher U values and widens. On the other hand, looking at Fig. 1(c), it appears that, within

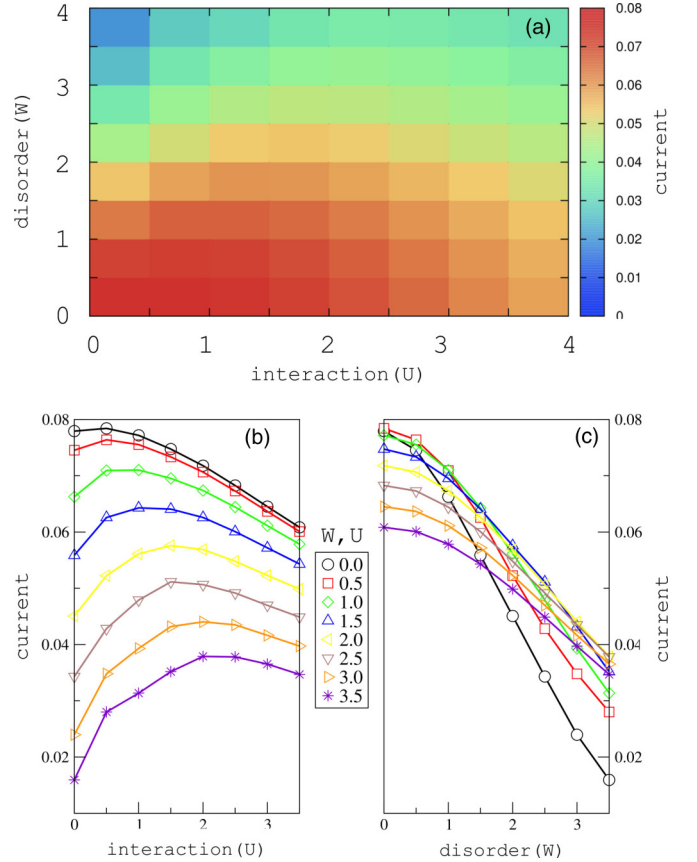


FIG. 1. (Color online) The effect of interactions and disorder on the current for a bias $b_L = 0.5$. (a) Heat map for the current. (b) Cuts along a fixed disorder strength (horizontal cuts in the heat map) as a function of U . (c) Cuts along a fixed interaction strength (vertical cuts) as a function of W . In (b) and (c), the lines are a guide for the eye. The legend applies to both (b) and (c).

the region of parameters considered, for any fixed value of U , the current monotonically decreases as a function of disorder strength. This observation appears to be inconclusive for higher W values since, quite interestingly, the spread of the current values reduces with increasing U and it is possible to note quite distinctly that the curvature changes at high U values.

The overall picture receives further support from the behavior of the differential conductance $\sigma = \frac{\delta I}{\delta b}$, obtained by numerical differentiation. In Fig. 2, we examine how σ scales with the size L of the central region. For $U = 0$ (solid and dashed red curves), we observe the expected exponential decrease in conductance. However, for $U > 0$, σ still decreases with increasing L , but in the interval of sizes considered, the trend is not as clear as for $U = 0$. An interesting feature in the equilibrium case is that when $W = 0$ and $U > 0$, σ is oscillatory. We have observed that these oscillations appear to be connected to the variance of the density with the same periodicity $L = 3m$ (with m an integer) and, on speculative grounds, this could be related to Friedel oscillations induced by the lead-chain-lead boundaries when $U > 0$. Coming now to the biased case, we recover the trends discussed earlier for $L = 10$, i.e., a competition between disorder and interaction

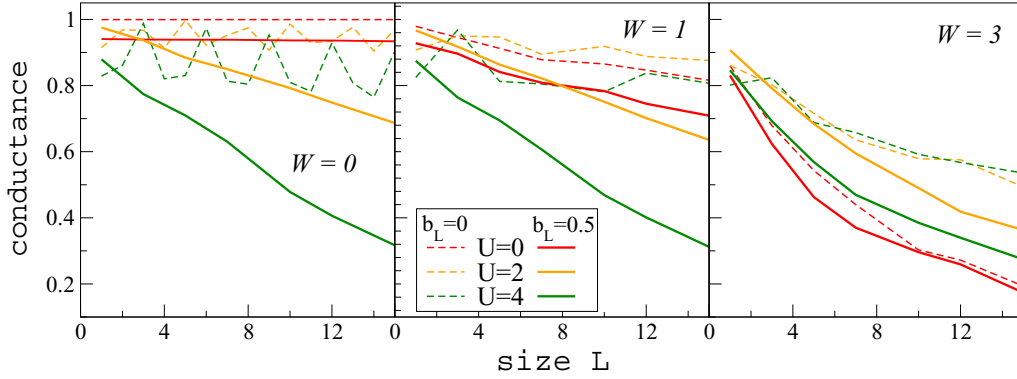


FIG. 2. (Color online) Averaged differential conductance $\sigma = dI/db$ as a function of the chain size L for box disorder and for bias $b_L = 0$ (dashed curves) and $b_L = 0.5$ (solid curves). The conductance is in units of the quantum of conductance.

which manifests as a nonmonotonic behavior of σ as a function of U . This is a robust feature for $W = 3$, present for all sizes considered, while for weaker disorder the trend in the dependence of σ on U also depends on the chain size.

The present results differ from a previous time-dependent density functional theory (DFT) treatment [32] where non-local correlation effects were neglected: The nonmonotonic trend in currents and conductances, missed in Ref. [32], stems from the ability of the BA to account for such effects.

The coherent potential approximation. We turn to another main topic of our work, namely, CPA out of equilibrium. CPA treats the disorder-averaged system by an effective medium, chosen so that the average t matrix of the local scatterer $\langle t_i(\omega) \rangle = 0$. This fulfills in an approximate way the constraint that, on average, the scattering matrix $\langle T \rangle = 0$ [33]. The equilibrium CPA condition is

$$\langle t_i(\omega) \rangle = \left\langle \frac{V_i - \Sigma_{ii}^{\text{CPA}}(\omega)}{1 - [V_i - \Sigma_{ii}^{\text{CPA}}(\omega)] G_{ii}(\omega)} \right\rangle = 0. \quad (9)$$

Here, V_i and $G_{ii}(\omega)$ are the impurity level and the averaged local propagator, respectively. This is how, in ground-state calculations, the complex, local in space, energy-dependent CPA self-energy Σ^{CPA} can be found.

Nowadays, by combining CPA with DFT in a NEGF self-consistent scheme, *ab initio* simulations of transport in realistic disordered systems are feasible [10,11]. On the other hand, *ab initio* NEGF treatments where CPA is combined with self-energies based on many-body approximations are still lacking. It is thus very timely and useful to assess CPA's performance when out of equilibrium and its conserving properties as a theory.

Usually, a conserving self-energy scheme for NEGF results from the existence of a so-called Φ functional [34], which guarantees particle, energy, and momenta conservation. As far as we know, such a functional has yet to be found for the CPA, and we here take a different route to rigorously prove that particle current is explicitly conserved out of equilibrium. This can be done either by reformulating Eq. (9) in terms of a set of auxiliary equations which are then reinterpreted as relations on the Keldysh contour [35], or by directly using the Langreth rules to extract the different components on the contour from Eq. (9). Either way, if we schematically

rewrite (site indexes and frequency arguments are omitted for simplicity) Eq. (9) as $c = (1 - ab)^{-1}a = 0$, then one can show that the retarded component $c^R = (1 - a^R b^R)^{-1} a^R$ and, for the lesser one, $c^< = (1 - a^R b^R)^{-1} a^< (1 - a^A b^A)^{-1} + c^R b^< c^A$. The Langreth rules for the retarded part give the CPA condition

$$0 = \langle t^R \rangle = \left\langle \frac{V - \Sigma_{\text{CPA}}^R}{1 - (V - \Sigma_{\text{CPA}}^R) G^R} \right\rangle, \quad (10)$$

while for the lesser/greater parts of Σ_{CPA} one arrives at

$$\Sigma_{\text{CPA}}^{<,>} = G^{<,>} \frac{\langle |t^R|^2 \rangle}{\left\langle \left| \frac{1}{1 - (V - \Sigma_{\text{CPA}}^R) G^R} \right|^2 \right\rangle}, \quad (11)$$

i.e., $\Sigma_{\text{CPA}}^{<,>} = G^{<,>} f(G^R, \Sigma_{\text{CPA}}^R)$, with f a real non-negative function. Equation (11) is valid for any noncorrelated disorder distribution. Except for noninteracting systems, Eqs. (10) and (11) must be solved together.

Using Eq. (8), the current difference ΔI becomes [36]

$$\Delta I = \int_{-\infty}^{\infty} \frac{d\omega}{2\pi} \text{Tr}[\Sigma_c^< G^> - \Sigma_c^> G^<], \quad (12)$$

where $\Sigma_c = \Sigma - \Sigma_{\text{emb}}$ refers to self-energy parts beyond the embedding self-energies. For a conserving approximation, $\Delta I = 0$. We first consider mean-field-type interactions, which means that $\Sigma_c^{<,>} = \Sigma_{\text{CPA}}^{<,>}$. Using Eq. (11), the integrand of Eq. (12) becomes

$$\begin{aligned} & \sum_i (\Sigma_{\text{CPA}}^<)_{ii} G_{ii}^> - (\Sigma_{\text{CPA}}^>)_{ii} G_{ii}^< \\ & = \sum_i G_{ii}^< f_i G_{ii}^> - G_{ii}^> f_i G_{ii}^< = 0. \end{aligned} \quad (13)$$

This holds for any number of leads, any type of (uncorrelated) disorder, and also when interactions are described with a mean-field-type self-energy, e.g., Hartree-Fock or Kohn-Sham DFT. To include interactions beyond mean field, we treat the self-energies as additive, i.e., $\Sigma_c = \Sigma_{\text{CPA}} + \Sigma_{\text{MB}}$. The BA is, by itself, a conserving scheme. However, when CPA (for which the existence of a Φ is not obvious) and BA are combined, particle conservation needs to be proven explicitly. We again use Eqs. (12) and (13), this time only for Σ_{MB} . This is more

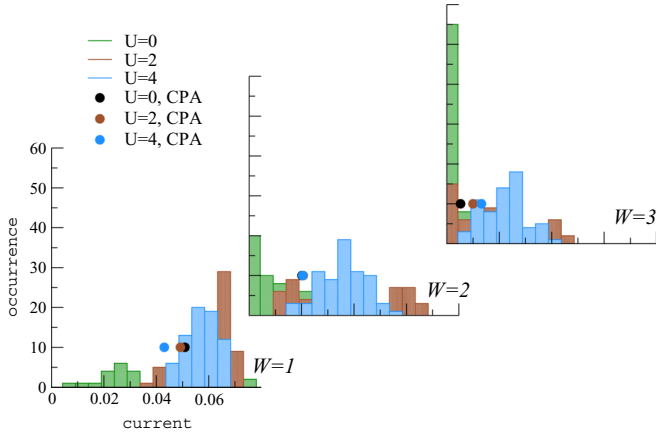


FIG. 3. (Color online) Steady-state currents for eight-site chains with binary disorder ($A_{50}B_{50}$ alloy) as a function of disorder and interaction strength. The applied bias $b_L = 0.5$. Both results for the exact distribution of currents (histograms) and CPA current averages (circles) are shown, discussed in the main text.

conveniently done in time space [Eq. (7)], where ΔI becomes

$$\Delta I = \int_{-\infty}^{\infty} dt \text{Tr}[\Sigma_{\text{MB}}^{\leftarrow}(t)G^{\rightarrow}(-t) - \Sigma_{\text{MB}}^{\rightarrow}(t)G^{\leftarrow}(-t)]. \quad (14)$$

Using the symmetries $G_{kl}^{\leftarrow,\rightarrow}(-t) = -[G_{lk}^{\leftarrow,\rightarrow}(t)]^*$, we get

$$\Delta I = 2i \sum_{kl} U_k U_l \int_{-\infty}^{\infty} dt \text{Im}\{[G_{kl}^{\leftarrow}(t)]^2 [(G_{kl}^{\rightarrow}(t))^*]^2\}. \quad (15)$$

Thus ΔI is cast as a purely imaginary expression. However, all reasonable approximations give real currents and the entire expression must vanish, i.e., CPA + BA is particle conserving. Our numerical calculations confirm that at self-consistency $\Delta I = 0$. However, in the initial self-consistency cycles, far away from convergence, we found that $\Delta I/I \approx 1$, i.e., self-consistency for CPA is crucial in quantum transport. Having shown the conceptual foundation of CPA for nonequilibrium treatments, we briefly discuss its performance in practice. By investigating short chains with binary disorder, we found that CPA, at least for the systems considered, can perform rather poorly and can in fact be unreliable even at the qualitative level. As an example, in Fig. 3 we report the distribution of currents for an eight-site chain with 50% binary disorder. As in Fig. 1, increasing the interactions reduces the role of disorder, and thus the typical value of the current (i.e., the

TABLE I. The spread of \mathcal{E}_k for different values of the bias and the disorder strength, in units of 10^{-3} . The minimum values of the spread are in bold.

	$U = 0$	$U = 1$	$U = 2$	$U = 4$
$W = 1, b_L = 0.0$	1.4	2.4	3.8	4.7
$W = 1, b_L = 0.5$	2.3	0.81	2.1	3.4
$W = 2, b_L = 0.0$	13	11	18	17
$W = 2, b_L = 0.5$	17	6.3	10	14

maximum value of the distribution) generally occurs at higher values. For $W = 1, 2$ it is also true that if U is further increased (i.e., $U = 4$), the current diminishes again. In any case, CPA currents are quantitatively incorrect, and only provide the correct qualitative picture for larger disorder $W = 3$.

Entanglement, disorder, and conductance. Recently, there has been an increasing interest in the use of entanglement entropy to characterize disordered interacting systems in equilibrium [21,22]. Here, we are interested in the nonequilibrium case, and specifically consider the single-site entanglement entropy \mathcal{E} , defined (in equilibrium) for site k [37] as $\mathcal{E}_k = -\sum_{\mu,\nu=+,-} \langle \hat{X}_{k\uparrow}^{\mu} \hat{X}_{k\downarrow}^{\nu} \rangle \log_2 \langle \hat{X}_{k\uparrow}^{\mu} \hat{X}_{k\downarrow}^{\nu} \rangle$, where $\hat{X}_{k\sigma}^+ = c_{k\sigma}^\dagger c_{k\sigma}$ and $\hat{X}_{k\sigma}^- = 1 - \hat{X}_{k\sigma}^+$. The expression for \mathcal{E}_k is straightforwardly generalized to finite biases. It is readily seen that \mathcal{E}_k can be expressed in terms of the particle density $n_k = \langle \hat{X}_{k\uparrow}^+ + \hat{X}_{k\downarrow}^+ \rangle$, obtained via $G^<$, and the double occupancy $d_k = \langle \hat{X}_{k\uparrow}^+ \hat{X}_{k\downarrow}^+ \rangle$. For the latter, we take the steady-state limit of the expression for the time-dependent double occupancy given in Ref. [38] and, for numerical convenience, separate the Hartree-Fock part:

$$d_k = \frac{n_k^2}{4} + \frac{1}{U_k} \int_{-\infty}^{\infty} \frac{d\omega}{2\pi i} (\Sigma_{\text{MB}}^{\leftarrow} G^A + \Sigma_{\text{MB}}^R G^{\leftarrow})_{kk}. \quad (16)$$

We have examined different sets of W, U, b_L parameters and their effect on \mathcal{E}_k . A convenient way to scrutinize the behavior is, for each set of parameters, to collect the pairs (n_k, \mathcal{E}_k) from all sites and disorder configurations, and arrange them in a cumulative histogram. In Fig. 4 we show histograms for the cases $U = 0, 2, 4$ when $W = 2$ and $b_L = 0.5$. In the noninteracting case, \mathcal{E}_k is completely determined by n_k . For interacting systems, $\mathcal{E}_k(n_k)$ is multivalued. It is apparent that, on increasing U , the spread of densities is reduced, and the densities are shifted to lower values. Similarly, \mathcal{E}_k shifts to lower values. More in general, studying other sets of parameters (as shown in Table I) we found that the main effect

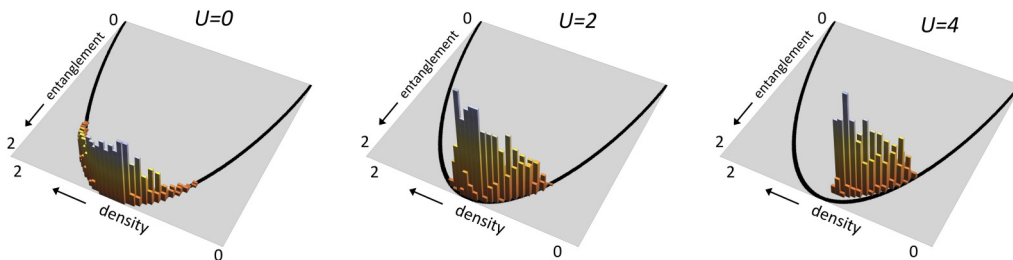


FIG. 4. (Color online) Cumulative distribution of the single-site entanglement entropy \mathcal{E}_k as a function of the interaction strength for a ten-site chain with $W = 2$ and bias $b_L = 0.5$. The black solid curves at the base of the entanglement histograms correspond to \mathcal{E}_k for a noninteracting system, i.e., $\langle \hat{X}_{k\uparrow}^{\mu} \hat{X}_{k\downarrow}^{\nu} \rangle = \langle \hat{X}_{k\uparrow}^{\mu} \rangle \langle \hat{X}_{k\downarrow}^{\nu} \rangle$, where $n_k \in [0, 2]$ and $\mathcal{E}_k \in [0, 2]$.

of increasing W is to increase the spread of the distributions, while applying a bias results in a shift of the density towards higher values. The spread of the distributions has, in the biased case, a similar type of nonmonotonicity as the current.

For each histogram in Fig. 4, we also calculated the variance of \mathcal{E}_k , and this is smallest for $U = 2$. Since these parameters correspond to a crossover case in Figs. 1 and 2, this suggests a possible connection between the nonmonotonic behavior of currents (or conductances) and the single-site entanglement entropy, i.e., the latter could be an indicator of the competition between disorder and interactions.

Conclusions. By means of NEGF, we investigated short disordered Hubbard chains contacted to leads to address questions regarding particle currents, conductances, and entanglement in quantum transport. We find that, in the presence of an electric bias, interactions can increase the current through a disordered system connected to macroscopic leads, but increasing interactions further can decrease the current

again. Our work generalizes to the quantum transport case the qualitative equilibrium picture for uncontacted systems with homogeneous disorder and interactions, and partially supports previous mean-field-type treatments for transport geometries. We have also shown that, out of equilibrium, the spread of entanglement entropy exhibits the same crossover as for currents and conductances. Finally, we gave a proof that CPA out of equilibrium is particle conserving, with or without electron correlations on the level of second-Born. This puts nonequilibrium CPA on conceptually firm ground, and sets the stage for considering electron correlations and disorder on equal footing in *ab initio* theories of systems out of equilibrium.

We thank Miroslav Hopjan for stimulating discussions. We also wish to acknowledge useful conversations with Herve Ness and Carl-Olof Almbladh. This work is supported by the Royal Physiographic Society in Lund.

-
- [1] E. Morosan, D. Natelson, A. H. Nevidomskyy, and Q. M. Si, *Adv. Mater.* **24**, 4896 (2012).
 - [2] *50 Years of Anderson Localization*, edited by E. Abrahams (World Scientific, Singapore, 2010).
 - [3] E. Abrahams, P. W. Anderson, D. C. Licciardello, and T. V. Ramakrishnan, *Phys. Rev. Lett.* **42**, 673 (1979).
 - [4] B. Kramer and A. MacKinnon, *Rep. Prog. Phys.* **56**, 1469 (1993).
 - [5] V. Dobrosavljevic and G. Kotliar, *Phys. Rev. Lett.* **78**, 3943 (1997).
 - [6] D. A. Rowlands, *Rep. Prog. Phys.* **72**, 086501 (2009).
 - [7] V. Drchal, *J. Phys. Chem. Solids* **40**, 393 (1979).
 - [8] W. M. Temmerman, B. L. Gyorffy, and G. M. Stocks, *J. Phys. F* **8**, 2461 (1978).
 - [9] M. Ye. Zhuravlev, A. V. Vedyayev, K. D. Belashchenko, and E. Y. Tsybal, *Phys. Rev. B* **85**, 115134 (2012).
 - [10] A. V. Kalitsov, M. G. Chshiev, and J. P. Velev, *Phys. Rev. B* **85**, 235111 (2012).
 - [11] Y. Zhu, L. Liu, and H. Guo, *Phys. Rev. B* **88**, 205415 (2013).
 - [12] R. T. Scalettar, in *Lectures on the Physics of Strongly Correlated Systems XI*, edited by A. Avella and A. Mancini, AIP Conf. Proc. No. 918 (AIP, Melville, NY, 2007), p. 111.
 - [13] P. J. H. Denteneer, R. T. Scalettar, and N. Trivedi, *Phys. Rev. Lett.* **83**, 4610 (1999).
 - [14] P. J. H. Denteneer, R. T. Scalettar, and N. Trivedi, *Phys. Rev. Lett.* **87**, 146401 (2001).
 - [15] J. T. Edwards and D. J. Thouless, *J. Phys. C* **5**, 807 (1972).
 - [16] T. Vojta, F. Epperlein, and M. Schreiber, *Phys. Rev. Lett.* **81**, 4212 (1998).
 - [17] A. Uppstu, Z. Fan, and A. Harju, *Phys. Rev. B* **89**, 075420 (2014).
 - [18] K. Byczuk, W. Hofstetter, and D. Vollhardt, *Int. J. Mod. Phys. B* **24**, 1727 (2010).
 - [19] J. Wernsdorfer, G. Harder, U. Schollwoeck, and W. Hofstetter, [arXiv:1108.6057](https://arxiv.org/abs/1108.6057).
 - [20] N. C. Murphy, R. Wortis, and W. A. Atkinson, *Phys. Rev. B* **83**, 184206 (2011).
 - [21] R. Berkovits, *Phys. Rev. Lett.* **108**, 176803 (2012).
 - [22] T. Br unner, E. Runge, A. Buchleitner, and V. V. Franca, *Phys. Rev. A* **87**, 032311 (2013).
 - [23] A. Kawabata, *Rep. Prog. Phys.* **70**, 219 (2007).
 - [24] L. P. Kadanoff and G. Baym, *Quantum Statistical Mechanics* (Benjamin, New York, 1962).
 - [25] L. V. Keldysh, *Sov. Phys. JETP* **20**, 1018 (1965).
 - [26] S. Datta, *Electronic Transport in Mesoscopic Systems* (Cambridge, England, 1995).
 - [27] P. My h nen, A. Stan, G. Stefanucci, and R. van Leeuwen, *Europhys. Lett.* **84**, 67001 (2008).
 - [28] M. Puig von Friesen, C. Verdozzi, and C.-O. Almbladh, *Phys. Rev. Lett.* **103**, 176404 (2009).
 - [29] S. Hermanns, N. Schl nzen, and M. Bonitz, *Phys. Rev. B* **90**, 125111 (2014).
 - [30] A.-M. Uimonen, E. Khosravi, A. Stan, G. Stefanucci, S. Kurth, R. van Leeuwen, and E. K. U. Gross, *Phys. Rev. B* **84**, 115103 (2011).
 - [31] Y. Meir and N. S. Wingreen, *Phys. Rev. Lett.* **68**, 2512 (1992).
 - [32] V. Vetchinkina, A. Kartsev, D. Karlsson, and C. Verdozzi, *Phys. Rev. B* **87**, 115117 (2013).
 - [33] P. Soven, *Phys. Rev.* **156**, 809 (1967).
 - [34] G. Baym, *Phys. Rev.* **127**, 1391 (1962).
 - [35] M. Hopjan and P. Lipavsk y, *Phys. Rev. B* **89**, 094507 (2014).
 - [36] K. S. Thygesen and A. Rubio, *Phys. Rev. B* **77**, 115333 (2008).
 - [37] D. Larsson and H. Johannesson, *Phys. Rev. Lett.* **95**, 196406 (2005).
 - [38] M. Puig von Friesen, C. Verdozzi, and C.-O. Almbladh, *EPL* **95**, 27005 (2011).